



## Full Length Article

# Enhancing the ignition, combustion, and propulsion performances of Al/CuO-based energetic materials incorporating with fullerene and carbon black particles

Abdul Basyir<sup>a</sup>, Ho Sung Kim<sup>b</sup>, Jung Keun Cha<sup>b</sup>, Soo Hyung Kim<sup>a,b,c,\*</sup>

<sup>a</sup> Department of Nanofusion Technology, College of Nanoscience and Nanotechnology, Pusan National University, Busandaehak-ro 63beon-gil, Geumjeong-gu, Busan 46241, Republic of Korea

<sup>b</sup> Research Center for Energy Convergence Technology, Pusan National University, Busandaehak-ro 63beon-gil, Geumjeong-gu, Busan 46241, Republic of Korea

<sup>c</sup> Department of Nanoenergy Engineering, College of Nanoscience and Nanotechnology, Pusan National University, Busandaehak-ro 63beon-gil, Geumjeong-gu, Busan 46241, Republic of Korea

## ARTICLE INFO

## Keywords:

Aluminum  
Copper Oxide  
Fullerene  
Carbon Black  
Combustion  
Propulsion

## ABSTRACT

This study investigated the effects of incorporating fullerene (C<sub>60</sub>) and carbon black (CB) particles into Al/CuO-based energetic materials (EMs) to enhance their ignition, combustion, and propulsion performances. EMs require high energy densities and rapid ignition characteristics for use as fuel in small projectiles. The systematic results indicated that the influences of C<sub>60</sub> and CB on the combustion performances of the EMs varied depending on their respective ratios. The optimal amounts of C<sub>60</sub> and CB enhanced the thermal properties of the Al/CuO-based EMs, increasing the levels of total heat energy release and subsequently accelerating the burn rates. The optimal carbon material (CM) ratio of approximately 1 wt% enhanced the handling safeties, burn rates, and explosion pressures of the Al/CuO-based EMs. CB addition resulted in larger improvements in the ignition and combustion performances than C<sub>60</sub> addition owing to the superior thermal conductivity and excellent dispersibility of CB. Furthermore, propulsion studies revealed that the optimal amount of CMs (approximately 1 wt %) improved the propulsion performance of the EMs, indicating the potential of CMs for use as effective control agents in projectile propulsion. However, excessive CM contents (>1 wt%) within the EMs hindered the aluminothermic reaction between Al and CuO, leading to decreases in the combustion performances. This study presents a novel approach for optimizing the combustion performances of EMs using CMs as effective additives, serving as a valuable foundation for the future application of small projectiles and energetic systems.

## 1. Introduction

Energetic materials (EMs) release high thermal energies upon ignition and combustion because of their fuel and oxidizer mixing ratios. EMs find applications in various thermal energy sources, explosives, and ammunition in different thermochemical engineering fields [1–6]. Among the various chemical compositions of EMs, Al is commonly used as a fuel, and CuO is frequently employed as an oxidizer. Al is widely utilized due to its relatively low density (approximately 2.7 g/cm<sup>3</sup>), high exothermic energy release, affordability, and availability [7,8]. Meanwhile, CuO is a potential oxidizer that induces high-temperature combustion when reacting with Al, enhances combustion efficiency, and exhibits stable properties at a relatively low cost [9,10].

Various carbon materials (CMs) recently attracted significant attention as additives for use in enhancing the ignition, combustion, and propulsion performances of EMs owing to their unique physical, thermal, electrical, and mechanical properties [11–13]. Pal et al. [14] reported that the addition of carbon black (CB) to paraffin-based hybrid rocket fuels improves their mechanical strengths and elastic moduli. They also observed an increase in the hardness of the fuel and an improved thermal stability via thermogravimetric analysis owing to the strong interactions of CB within the paraffin matrix. Han et al. [15] combined CB or fullerenes (C<sub>60</sub>) with cyclotrimethylenetrinitramine (RDX)-based propellants to observe their combustion characteristics, and the inclusion of CB within the RDX-based propellant produced a higher combustion rate than that observed when C<sub>60</sub> was added. Jin

\* Corresponding author at: Department of Nanofusion Technology, College of Nanoscience and Nanotechnology, Pusan National University, Busandaehak-ro 63beon-gil, Geumjeong-gu, Busan 46241, Republic of Korea.

E-mail address: [sookim@pusan.ac.kr](mailto:sookim@pusan.ac.kr) (S.H. Kim).

<https://doi.org/10.1016/j.fuel.2025.134688>

Received 25 October 2024; Received in revised form 12 December 2024; Accepted 9 February 2025

Available online 13 February 2025

0016-2361/© 2025 Elsevier Ltd. All rights are reserved, including those for text and data mining, AI training, and similar technologies.

**Table 1**

Various Al/CuO/CM composites fabricated using liquid mixing and secondary drying.

Sample	Al (wt.%)	CuO (wt.%)	CM (wt.%)
Al/CuO	30.00	70.00	0.0
Al/CuO/CM0.5	29.85	69.65	0.5
Al/CuO/CM1	29.70	69.30	1.0
Al/CuO/CM2.5	29.25	68.25	2.5
Al/CuO/CM5	28.50	66.50	5.0
Al/CuO/CM10	27.00	63.00	10.0

et al. [16] observed decreases in the friction and impact sensitivities of cyclotetramethylene tetranitramine (HMX) when 1 wt% C<sub>60</sub> was added to the solid HMX propellant. However, these previous studies fixed the mass of the CM to a specific amount and did not investigate the optimal quantity of the CM. They were limited to the measurement of basic thermal and combustion properties without systematically observing the changes in propellant performance when applied as rocket fuels. Consequently, systematic studies regarding the effects of traditional OD CMs, such as C<sub>60</sub> and CB, on the ignition, combustion, and propulsion characteristics of EMs are rare. In addition to OD CMs, Wang et al. [17], Jiang et al. [18], and Shen et al. [19] utilized 1D carbon fibers, 2D graphene oxide, and graphene, respectively, as additives in an Al/CuO-based EM matrix and observed improvements in the burn rate, thermal energy release, and overall combustion performance. Similarly, Su et al. [20] and Chen et al. [21] incorporated 2D graphene oxide into an Al/CuO-based EM matrix and reported an approximately two-fold increase in the exothermic energy of the EMs. However, these studies also fixed the amount of CM added and were limited to observing changes in the basic combustion characteristics without systematically studying the ignition, combustion, and propulsion characteristics.

In this study, we selected C<sub>60</sub> and CB, which are two representative CMs with identical carbon compositions but different physical forms and structures, and incorporated them into Al/CuO-based EMs. The objective of this study was to systematically investigate the combustion, explosion, and propulsion characteristics upon ignition. The unique structures and physical properties of C<sub>60</sub> and CB were examined in terms of their interactions with nanoscale Al/CuO-based EMs. We focused on the influence of these CMs on the combustion characteristics when mixed and integrated within the EMs and the effects of these changes in combustion behavior on the propulsion characteristics when utilized as solid propellants in small-scale projectiles. Al/CuO/CM-based EMs were prepared using wet chemistry-based liquid mixing and drying. We systematically measured the ignition sensitivities, burn rates, and explosion pressures of the Al/CuO-based EMs as functions of the added amounts of C<sub>60</sub> microparticles and CB nanoparticles. Finally, we loaded the Al/CuO/CM-based EMs into the combustion chambers of small bullet- and rocket-type projectiles, ignited them, and measured and analyzed the real-time propulsion characteristics of these small-scale projectiles.

## 2. Experimental Section

### 2.1. Fabrication of the Al/CuO/CM-based EMs

In this study, Al (fuel), CuO (oxidizer), and CMs (thermokinetic reaction control agents), i.e., C<sub>60</sub> and CB, were used as precursors of the EMs. Commercially available Al (purity: 99.9 %, CNVISION, Seoul, Republic of Korea), CuO (purity: 99.8 %, CNVISION), C<sub>60</sub> (purity: 98 %, Sigma-Aldrich, St. Louis, MO, USA), and CB (Ketjenblack EC-300 J, Akzo Nobel Functional Chemicals, Amsterdam, Netherlands) powders were purchased and used without further treatment. The mixing ratio of the metal fuel, Al, and oxidizer, CuO, was fixed at 30:70 wt% (i.e., fuel/oxidizer ratio  $\phi = 1.9$ ), and the CMs added to the Al/CuO-based EMs were mixed at mass percentages of 0.5, 1, 2.5, 5, and 10 wt%. The names and compositions of the Al/CuO/CM composites are listed in Table 1.

We employed conventional solution drying to prepare the Al/CuO/

CM composite powders. Each precursor material (Al, CuO, and CM) was dispersed in an ethanol solution (purity: 99.0 %, DUKSAN Pure Chemical, Ansan, Republic of Korea) and ultrasonicated (approximately 40 kHz, WUC-D03H, DAIHAN Scientific, Wonju, Republic of Korea) for approximately 30 min to ensure homogeneous mixing. The ethanol-dispersed colloidal solution of Al/CuO/CM was dried in an oven at 80 °C for approximately 15 min, and finally, the dried Al/CuO/CM-based EMs was collected.

### 2.2. Characterization of the thermophysical properties of the Al/CuO/CM-based EMs

The morphologies, compositions, surface areas, and thermal properties of the precursors and EMs were observed using various techniques: scanning electron microscopy (SEM, JSM-7900F, JEOL, Tokyo, Japan) operated at ~20 kV and combined with energy-dispersive X-ray spectroscopy (EDS, Ultim Max 100, Oxford Instruments, Abingdon, UK), Brunauer-Emmett-Teller (BET) N<sub>2</sub> gas adsorption analysis (Autosorb iQ, Anton Paar QuantaTec, Boynton Beach, FL, USA) [22,23], and differential scanning calorimetry (DSC, Labsys EVO 1600, SETARAM, Caluire-et-Cuire, France) operated from 30 to 1000 °C at a heating rate of 10 °C/min under flowing Ar gas.

### 2.3. Electrical discharge, friction sensitivity, and mechanical impaction studies of the Al/CuO/CM-based EMs

Electrostatic discharge (ESD) studies were conducted using an ESD simulator (KES4021, Kikusui Electronics, Yokohama, Japan) to evaluate the stabilities of the ESDs of the Al/CuO/CM-based EMs. Approximately 3 mg of the EM powder was placed 1 mm from the discharge gun (i.e., metal wire), which was connected to the ESD simulator with a capacitor capacitance of 330 pF. The applied potential range of the ESD simulator was 0–30 kV. To calculate the energy of the ESD, the formula  $E_E = 0.5CV^2$  was used, where  $E_E$ ,  $C$ , and  $V$  represent the discharge energy (mJ), capacitance (F), and input potential (V), respectively. The ignition threshold spark energy of the EMs, when ignition and explosion occurred therein upon artificial spark application, was determined as the observed spark energy of the evaluated sample with a 50 % probability of ignition.

A friction apparatus (FSA 12, OZM Research, Hrochův Týnec, Czechia) approved from German Federal Institute for Materials Research and Testing was used to measure the friction sensitivities of the EMs. A 10 mm<sup>3</sup> sample of the EMs was placed on the porcelain plate, and standard masses ranging from 5 to 360 N were alternately applied to the 6-position loading arm of the apparatus. The ignition threshold of the frictional force was determined as the frictional force at which the EMs ignited with a 50 % probability due to the standard mass.

To measure the sensitivity of the EMs to mechanical impact, composites, a manually operated free-falling hammer was used to impact pre-prepared metal stage-filled holes containing the EM powder (approximately 40 mg) [24,25]. The mechanical impact equipment was designed with a hammer (mass: 0.5 ~ 3 kg) secured at a maximum height of 200 cm to fall onto the EMs via gravity. When the EMs ignited and exploded at a specific potential energy applied by the hammer, lower mechanical impacts were repeatedly applied to observe the ignition and explosion. The ignition threshold mechanical impact energy ( $E_{MI} = mgh$ , where  $m$ ,  $h$ , and  $g$  are the mass and height of the hammer and gravitational acceleration, respectively) with a 50 % probability of ignition was thus determined.

### 2.4. Measurement of the ignition and combustion characteristics of the Al/CuO/CM-based EMs

A temperature jump (T-jump) wire device was used to measure the ignition delay of the EM powder. Initially, a Pt wire with a diameter of 75 μm was coated with the EM powder. The ignition wire was connected

**Table 2**

Types and compositions of KNSU and Al/CuO/CM used in the propulsion studies of the rocket-type projectiles.

Type of composite solid propellant	Mixing ratio of components in wt. %
KNSU–Al/CuO	$\text{KNO}_3:\text{C}_{12}\text{H}_{22}\text{O}_{11}:\text{Al}:\text{CuO}:\text{CM} = 65:35:0:0:0$
KNSU–Al/CuO/CM0.5	$\text{KNO}_3:\text{C}_{12}\text{H}_{22}\text{O}_{11}:\text{Al}:\text{CuO}:\text{CM} = 62.40:33.60:1.19:2.79:0.02$
KNSU–Al/CuO/CM1	$\text{KNO}_3:\text{C}_{12}\text{H}_{22}\text{O}_{11}:\text{Al}:\text{CuO}:\text{CM} = 62.40:33.60:1.19:2.77:0.04$
KNSU–Al/CuO/CM2.5	$\text{KNO}_3:\text{C}_{12}\text{H}_{22}\text{O}_{11}:\text{Al}:\text{CuO}:\text{CM} = 62.40:33.60:1.17:2.73:0.10$
KNSU–Al/CuO/CM5	$\text{KNO}_3:\text{C}_{12}\text{H}_{22}\text{O}_{11}:\text{Al}:\text{CuO}:\text{CM} = 62.40:33.60:1.14:2.66:0.20$
KNSU–Al/CuO/CM10	$\text{KNO}_3:\text{C}_{12}\text{H}_{22}\text{O}_{11}:\text{Al}:\text{CuO}:\text{CM} = 62.40:33.60:1.08:2.52:0.40$

to the T-jump probe, which was connected to the switching devices, current (TDS3012B, Tektronix, Beaverton, OR, USA) and voltage (TDS2012B, Tektronix) oscilloscopes, and a power supply (6 V). Signals were detected in the voltage and current oscilloscopes when the EM powder on the Pt wire was ignited, and the measured signal rise time at this point represented the ignition delay of the sample. To complement the measurements obtained using the T-jump probe system,

simultaneous measurements were performed utilizing a high-speed camera (FASTCAM SA3 120 K, Photron, Tokyo, Japan) operating at a frame rate of 30 000 fps.

To measure the burn rate of the EMs, approximately 150 mg of the powder was loaded into a cylindrical polyethylene terephthalate tube with a respective inner diameter and length of 1 and 70 mm. The tube was then inserted into a transparent acrylic block with a length of 40 mm. The EM powder was ignited at one end of the burn tube inserted into the acrylic block. The propagation of the combustion flame to the opposite end of the tube was then recorded in real time using the Photron high-speed camera (frame rate: 50 000 fps) to measure the burn rate.

A pressure cell test (PCT) was conducted to investigate the explosion pressure of the EM powder (test quantity: ~13 mg). The PCT system comprised a W hot-wire igniter (supply current: ~2 A, supply potential: ~4 V), closed stainless-steel (SUS304) cell with a constant volume (~13 mL), pressure sensor with a sensitivity of 14.5 mV/kPa (113B28, PCB Piezotronics, Depew, NY, USA), signal conditioner (482C series, PCB Piezotronics), and digital oscilloscope (TDS2012B, Tektronix). A real-time graph of the time-pressure relationship during the ignition of the EM powder was measured, based on which the pressurization rate was also determined. The pressurization rate refers to the maximum pressure generated during the ignition of the EMs divided by the time

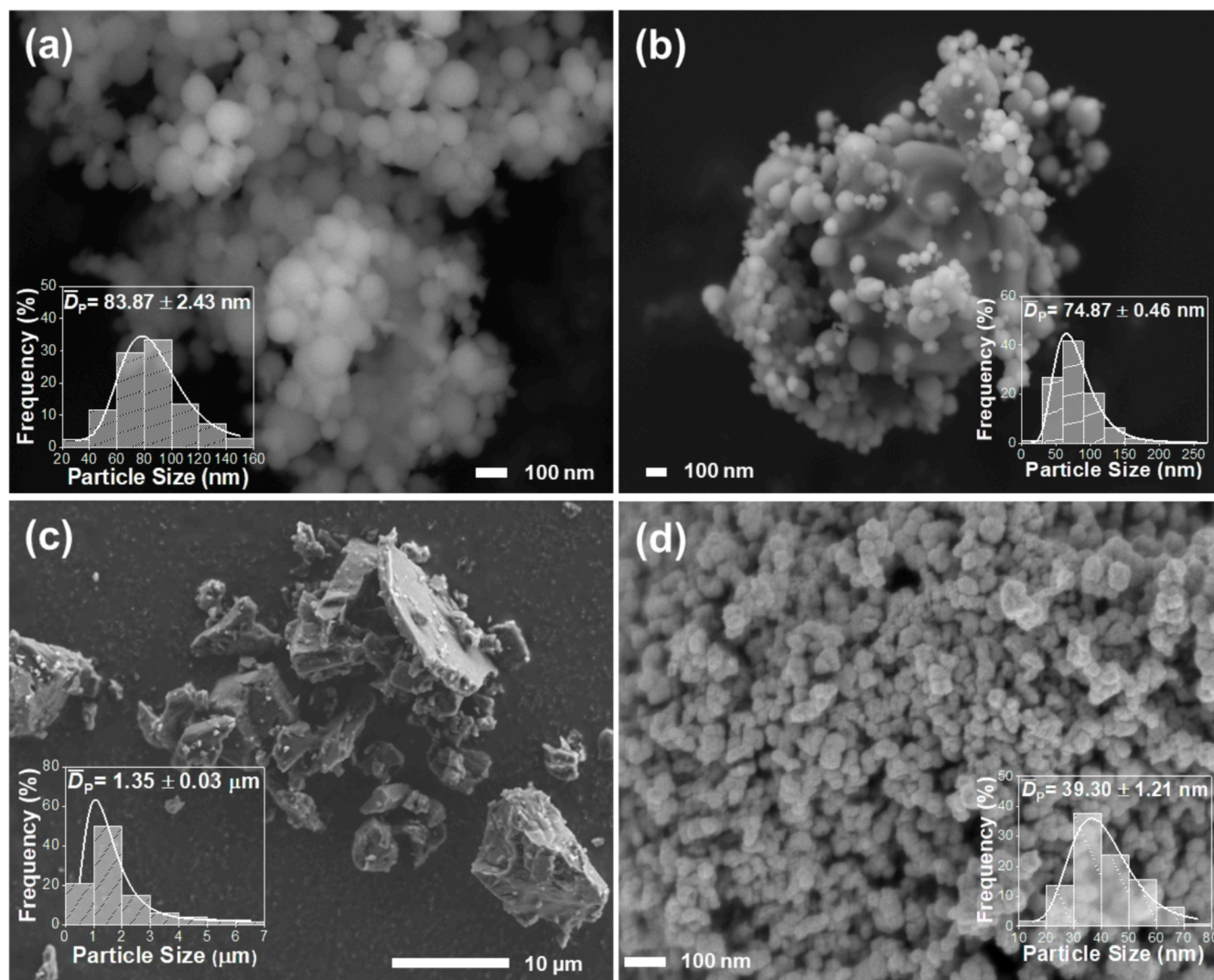


**Fig. 1.** High-resolution scanning electron microscopy images of the (a) Al, (b) CuO, (c) fullerene ( $\text{C}_{60}$ ), and (d) carbon black (CB) precursor materials employed in this study (Insets are the particle size distributions).



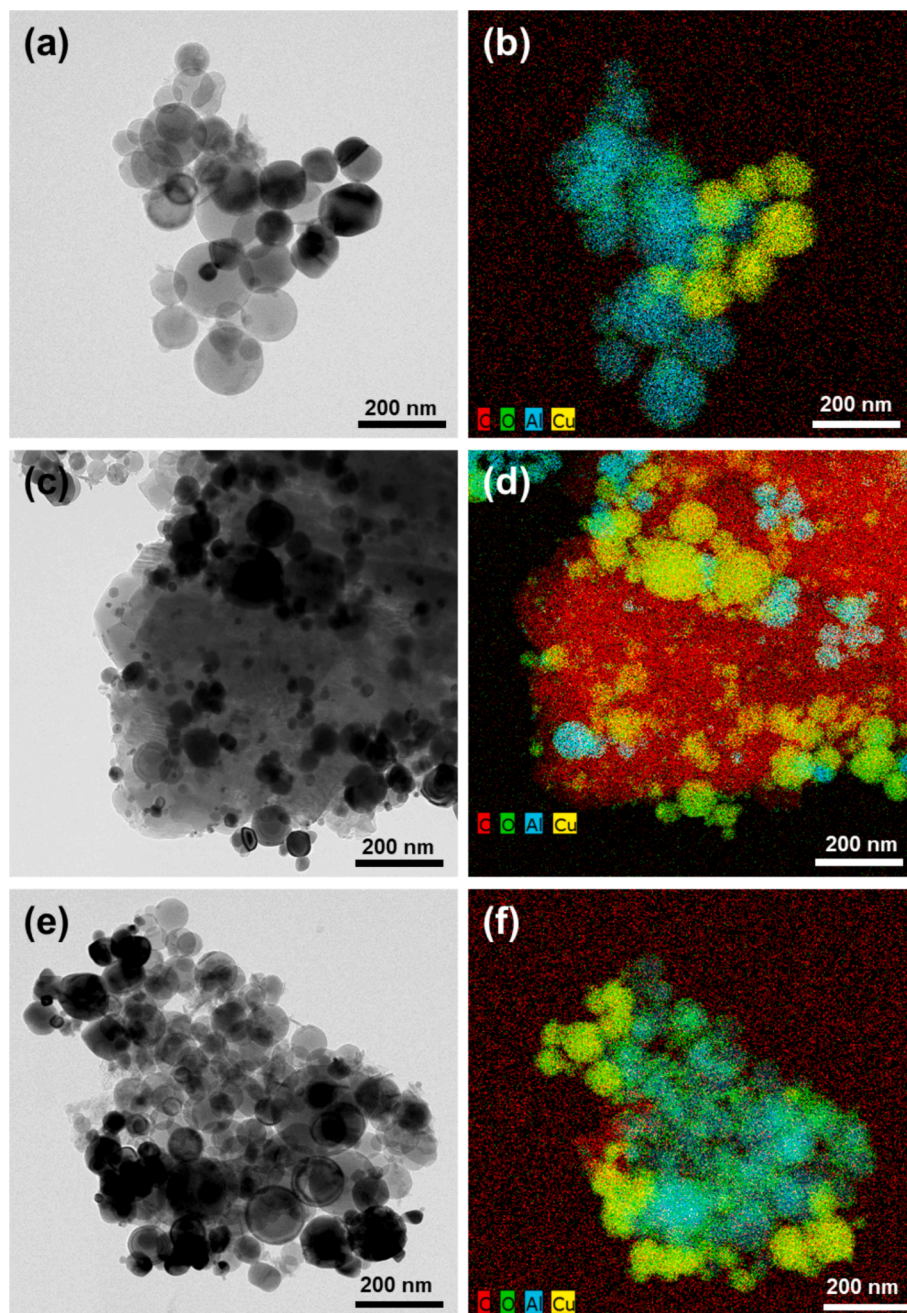


**Fig. 2.** High-resolution transmission electron microscopy images and energy-dispersive X-ray spectroscopy elemental mapping of (a, b) Al/CuO, (c, d) Al/CuO/C<sub>60</sub>, and (e, f) Al/CuO/CB.

required to reach that pressure.

### 2.5. Propulsion studies of small projectiles charged with Al/CuO/CM-based EMs

The propulsion characteristics of the EM powders were initially determined using a bullet-type small projectile launcher. The specifications of the SUS304 bullet-type small projectile were as follows: mass: 3.54 g; length: 2 cm; inner diameter: 0.74 cm; and outer diameter: 0.96 cm; and the specifications of the gun barrel comprised of a glass tube were as follows: length: 50 cm; inner diameter: 1 cm; and outer diameter: 1.3 cm. To measure the propulsion characteristics of the small bullet-type projectile, approximately 400 mg of the EM powder was loaded into the small bullet-type projectile, which was aligned at the entrance of the gun barrel. By igniting the primer at the end of the

projectile with a flame, the projectile was propelled rapidly within the gun barrel by the thrust generated during the combustion of the EM powder inside the bullet-type projectile. This motion was captured in real time using a high-speed camera to measure the average velocity of the projectile and calculate its kinetic energy. The average velocity of the projectile was determined by dividing the length of the gun barrel by the time required for the projectile to pass through it. The kinetic energy of the projectile was calculated using the formula  $E_K = 0.5mv^2$ , where  $E_K$ ,  $m$ , and  $v$  represent the kinetic energy (J), mass (kg), and average velocity (m/s) of the projectile, respectively.

Rocket-type small projectile propulsion studies were conducted to observe the propulsion characteristics of the EM powders. The prepared Al/CuO/CM-based EMs (Table 2) were applied as additives to a conventional solid propellant (i.e., KNO<sub>3</sub> (Daejung Chemicals & Metals, Siheung, Republic of Korea) and sucrose (C<sub>12</sub>H<sub>22</sub>O<sub>11</sub>, Sigma-Aldrich)



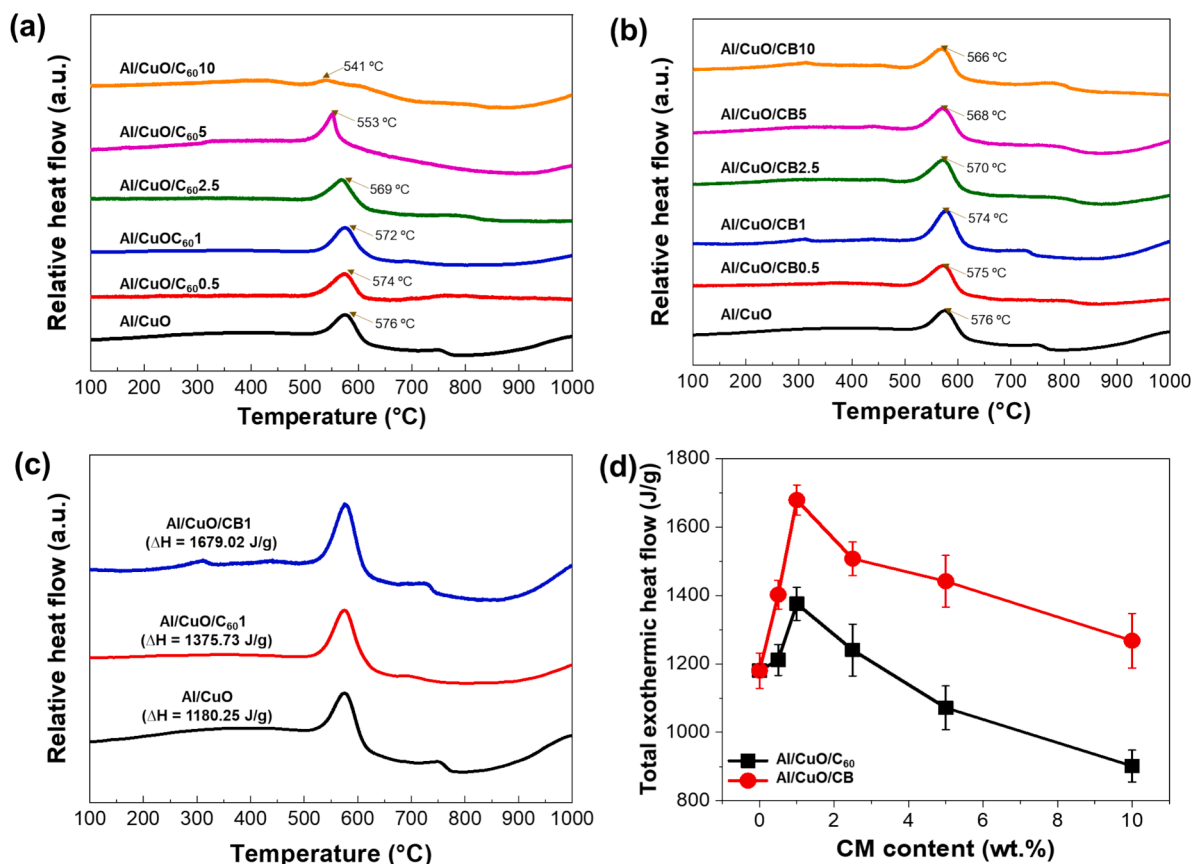


**Fig. 3.** Differential scanning calorimetry (DSC) thermograms of the various Al/CuO-based energetic materials (EMs) added with different amounts of (a) fullerene (C<sub>60</sub>) and (b) carbon black (CB). (c) Comparison of the DSC thermograms and calculated total exothermic heat flows for the cases of Al/CuO, Al/CuO/C<sub>60</sub>1, and Al/CuO/CB1. (d) Total exothermic heat flows of the EMs as a functions of carbon material (CM) content.

physically mixed using a ball mill (LM-BD4530, LK Lab Korea, Namyangju, Republic of Korea) at 60 rpm for approximately 90 min at a ratio of KNO<sub>3</sub>:C<sub>12</sub>H<sub>22</sub>O<sub>11</sub> = 65:35 wt%, denoted KNSU hereafter). Various Al/CuO/CM and KNSU mixtures were compressed to approximately 8 g at 20 bar for 1 min in a small rocket motor, which was installed in a wind tunnel (width: 30 cm, height: 30 cm, length: 2 m), and then ignited and combusted using an igniter to generate thrust within the rocket motor. The resulting thrust of the rocket motor was measured using a load cell (PW2D, Hottinger, Brüel, & Kjær, Darmstadt, Germany) and data acquisition device (espressoDAQ, Hottinger, Brüel, & Kjær).

### 3. Results and discussion

According to the results of high-resolution SEM, as shown in Fig. 1, the precursor materials employed in this study—Al, CuO, and CB and C<sub>60</sub> as the fuel component, oxidizing agent, and agents used in controlling the thermochemical reactions, respectively—exhibit respective average diameters of  $83.87 \pm 2.43$ ,  $74.87 \pm 0.46$ , and  $39.30 \pm 1.21$  nm and  $1.38 \pm 0.03$   $\mu$ m. Al, CuO, and CB exhibit almost spherical shapes, whereas C<sub>60</sub> exhibits various irregular shapes. CB, which generally consists of amorphous C, contains numerous defects and active sites, whereas C<sub>60</sub> is characterized by a highly ordered structure, with fewer defects and a relatively low reactivity [26–28]. N<sub>2</sub> adsorption studies reveal that CB exhibits a >10-fold higher specific surface area (SSA) compared to that of C<sub>60</sub> (i.e.,  $SSA_{C_{60}} = 93.96$  m<sup>2</sup>/g,  $SSA_{CB} = 1138.32$  m<sup>2</sup>/g), which is because CB and C<sub>60</sub> respectively display nanometer- and micrometer-scale size distributions without any porous structures.

We conducted high-resolution transmission electron microscopy and EDS of the EMs formed by mixing the various precursor materials, and

the results are shown in Fig. 2. In the EMs comprising only Al and CuO without the CMs, the Al and CuO particles are closely attached well at the nanoscale (Fig. 2a and b). In the Al/CuO/C<sub>60</sub>-based EMs, nanosized Al and CuO particles are well-attached, forming spherical particles around the larger polyhedral C<sub>60</sub> on the microscale (Fig. 2c and d). In the Al/CuO/CB-based EMs, the three precursor materials are uniformly distributed (Fig. 2e and f). Based on the bonding states between the CM additives and Al/CuO-based EMs, the addition of CB (which exhibits a nanoscale size distribution) may facilitate more vigorous thermal energy release during the ignition and combustion of EMs compared to that facilitated by C<sub>60</sub> (which displays a microscale size distribution).

DSC was performed to observe the exothermic characteristics induced by CM addition to the Al/CuO-based EMs. As shown in Fig. 3a and b, the maximum exothermic temperature gradually decreases as the amount of the C<sub>60</sub> or CB additive within the EM increases. This is attributed to the enhancement of the thermal conductivity properties of the EM owing to CM addition. The thermal conductivity studies of the CMs used yield thermal conductivities of approximately 0.25 and 0.42 W/m•K for C<sub>60</sub> and CB, respectively. The areas under the exothermic DSC peaks shown in Fig. 3c were integrated. The results show that the total heat release significantly increases when C<sub>60</sub> or CB is added at 1 wt % within the Al/CuO-based EM compared to that of the EM without CM additives. Calculating the total heat release of the EM as a function of CM addition, as shown in Fig. 3d, reveals a substantial increase in the total heat release when the CM is added at 0.5–1.0 wt%, whereas a CM content of >1.0 wt% results in a sharp decrease. This indicates the necessity of experimentally determining the optimal amount of CM required to increase the total heat release from the EMs. Therefore, adding more than the optimal amount of CM may thermochemically interfere with the aluminothermic reaction between Al and CuO.

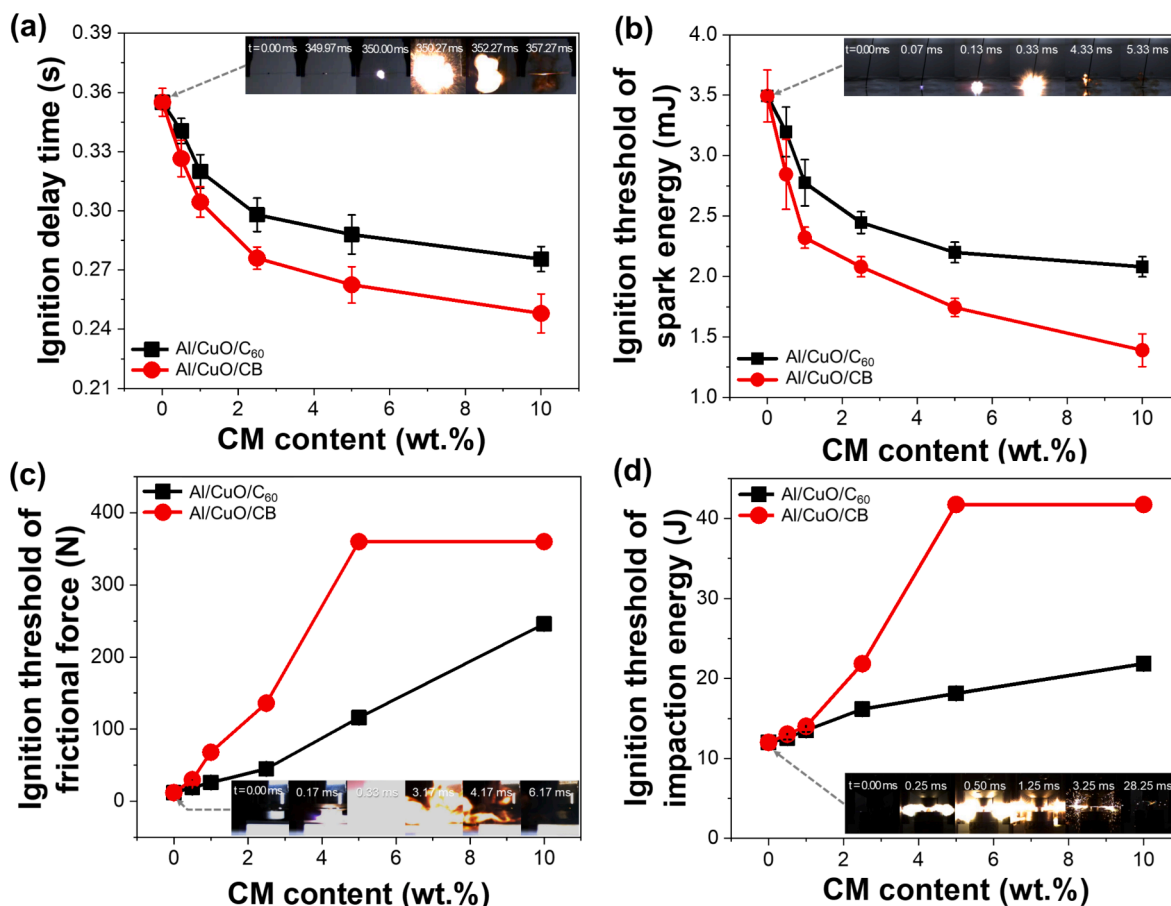


**Fig. 4.** (a) Ignition delay times and ignition thresholds of (b) spark energy, (c) frictional force, and (d) impact energy for Al/CuO-based energetic materials (EMs) doped with various amounts of carbon material (CM) (the insets show the sequential images of the Al/CuO-based EMs ignited using a temperature-jump wire, a spark caused by electrostatic discharge, and a frictional force and hammer impact, respectively).

Furthermore, the levels of total heat release of the EMs with CB additives clearly surpass those of the EMs with C<sub>60</sub> additives, despite containing the same C contents. This suggests that the potential utilization of diverse CM additives as thermochemical regulators in EMs depends on their thermal properties.

To observe changes in ignition characteristics of the Al/CuO-based EMs with varying amounts of CMs, the ignition delay times and ignition thresholds in terms of electrical sparks/frictional force/mechanical impact were measured, as shown in Fig. 4. Fig. 4a shows that the ignition delay times gradually decrease as the CM contents within the EMs increase. Upon applying a potential to a Pt wire (inset of Fig. 4a), localized heating occurs, and the EMs coated with CB, which displays a higher thermal conductivity than that of C<sub>60</sub>, exhibit relatively reduced ignition delay times. The ESD study (Fig. 4b) reveals that the ignition threshold of the spark energy decreases gradually with increasing CM content. The EM without CM additives exhibits a spark ignition threshold of 3.49 mJ, whereas Al/CuO/C<sub>60</sub>10 and Al/CuO/CB10 exhibit thresholds of 2.08 and 1.39 mJ, respectively. Thus, adding CB clearly reduces the ignition threshold more significantly than adding C<sub>60</sub> to the EMs, which is attributed to the higher electrical conductivity ( $\sigma$ ) of CB that facilitates the faster transmission of the applied electrical energy to the EMs ( $\sigma_{C60} = 10^{-10} - 10^{-5}$  S/m [29];  $\sigma_{CB} = 10^{-1} - 10^2$  S/m [30];  $\sigma_{Al/CuO} = 10^{-10} - 10^{-6}$  S/m [31]). However, the frictional force and mechanical impact ignition threshold measurements (Fig. 4c and d) indicate that increasing the CM content enhances the stability of the Al/CuO-based EMs. Whereas the composite without CM additives ignites easily under 10 N and 12.01 J of frictional force and mechanical impact energy, respectively, the ignition thresholds gradually increase with increasing CM content. CB addition, in particular, leads to higher

increases in the ignition thresholds of the EMs compared to those caused by C<sub>60</sub> addition, indicating enhanced frictional force and mechanical impact stabilities. This is attributed to the lower density of CB compared to that of C<sub>60</sub>, enabling the CB particles to envelop the composite more effectively at the same mass percentage, thereby protecting it from external frictional forces and mechanical impact. Moreover, the higher Young's modulus ( $Y$ ) of CB compared to that of C<sub>60</sub> ( $Y_{C60} \sim 0.05$  TPa [32];  $Y_{CB} \sim 0.08$  TPa [33];  $Y_{Al/CuO} \sim 0.001$  TPa [34]) suggests that CB more effectively absorbs and mitigates the external frictional force and mechanical impact on Al/CuO. These results indicate the importance of appropriately considering the addition of moderate amounts of CMs to Al/CuO-based EMs, as they can enhance the ignition characteristics while decreasing the electrical stabilities and improving the frictional force and mechanical impact stabilities.

To examine the effects of CM addition the burn rates of the Al/CuO-based EMs, a series of burn tube tests were also performed. Fig. 5a and b presents the schematic and photograph of the burn tube test system, respectively. Fig. 5c and d show the high-speed camera images of flame propagation of the Al/CuO-based EMs doped with various amounts of CM content. Commonly, when the CM is added at a level of approximately  $\leq 1$  wt%, the burn rate gradually increases as the CM content increases. Inversely, as the burn rate increases, the total burning time generally decreases (Fig. 5e and f). The burn rate was determined by dividing the distance from the inlet to the outlet of the burn tube by the time required for flame propagation, and the total burning time was determined by the total time it takes for the flame to travel from the inlet to the outlet of the burn tube. As shown in Fig. 5e and f, at approximately 1 wt% of added C<sub>60</sub> and CB, the maximum burn rates of the EMs are approximately 312.50 and 337.10 m/s, respectively. However, when

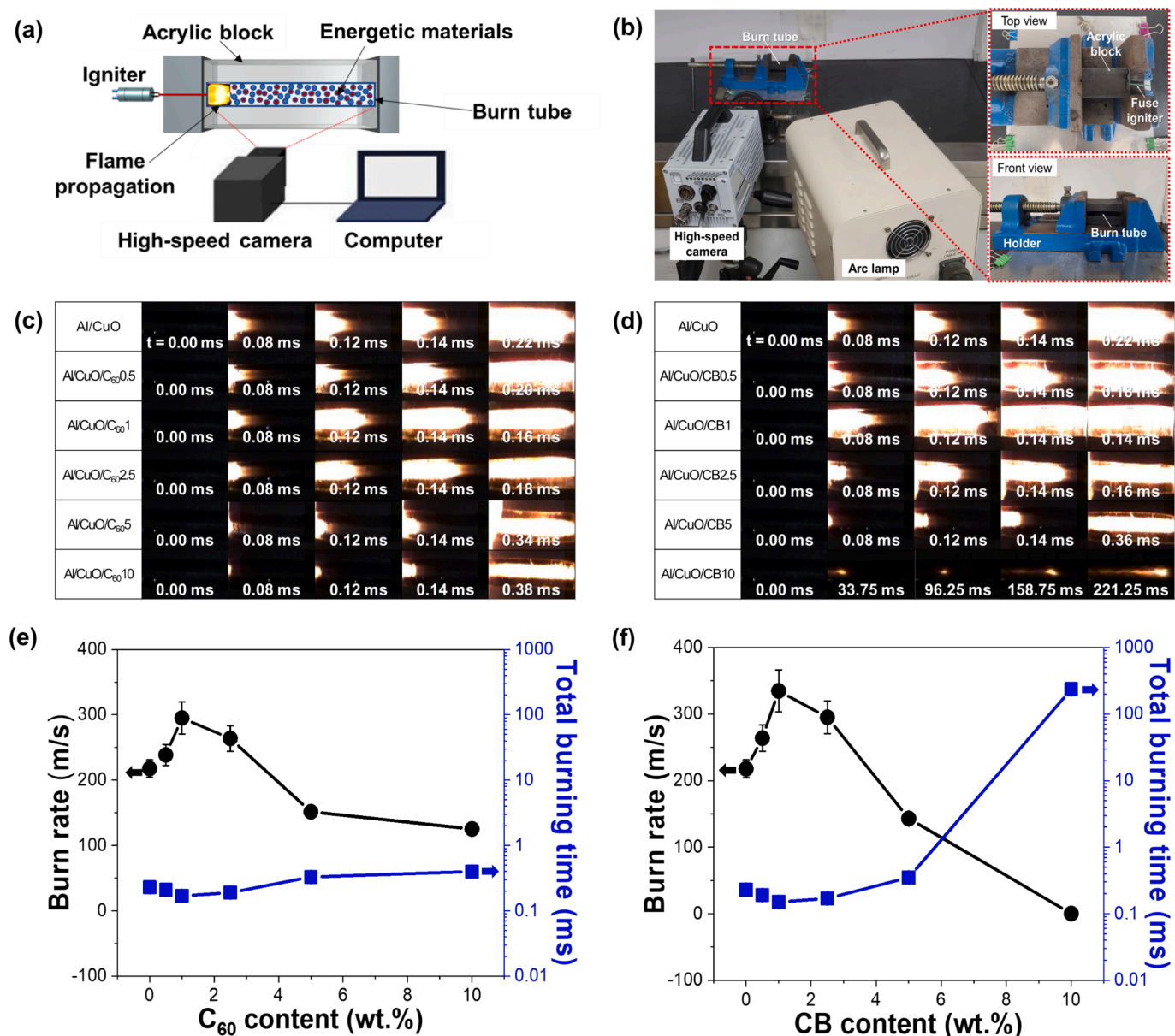


Fig. 5. (a) Schematic and (b) photograph of burn tube apparatus, and high-speed camera images of the combustion flame propagation of the (c) fullerene (C<sub>60</sub>)- and (d) carbon black (CB)-added Al/CuO energetic materials (EMs) incorporated with different carbon material contents in the burn tube. Evolution of burn rate and total burning time of the (e) C<sub>60</sub>- and (f) CB-doped Al/CuO-based EMs.

the CM contents are  $>1$  wt%, the burn rates of the EMs decrease sharply. Consequently, at up to a certain CM content, the burn rate of the EMs increases, whereas the total burning time decreases. However, adding excessive amounts of the CMs beyond the optimal amounts reduces the burn rates of the EMs, which is partially due to the CMs perturbing the aluminothermic reactions between Al and CuO within the EMs.

We measured the real-time changes in the explosion pressures within sealed pressure cells upon the artificial ignition of the Al/CuO-based EM powders with varying amounts of the CMs (Fig. 6a and b). The effects of CM addition on the explosion pressures of the EM powders during ignition were thus observed (Fig. 6c and d). The maximum explosion pressure and pressurization rate increase significantly when  $\leq 1$  wt% CM is added (Fig. 6e and f). The pressurization rate was calculated by dividing the maximum explosion pressure by the time required to reach it. Generally, the explosion pressure rapidly reaches its peak within an extremely short time and then decreases sharply. At high CM contents ( $>5$  wt%), the increases in the explosion pressures of the EMs are

relatively slow. Notably, similar to the previously observed results of the burn rate studies, the increases in the maximum explosion pressures and pressurization rates of the EMs are clearly more pronounced with CB addition compared to those observed with C<sub>60</sub> addition. This suggests that CB, with its superior heat transfer properties within the Al/CuO-based EM matrix, enhances the combustion reaction more effectively than C<sub>60</sub> when added in an appropriate amount. However, the excessive addition of the CMs ( $>5$  wt%) deteriorates the combustion characteristics of the EMs.

To observe the effects of CM addition on the propulsion characteristics of the EMs, we filled bullet-type projectiles with the EM powders containing various amounts of the CMs. After ignition, we recorded the motions of the bullet-type projectiles in cylindrical glass gun barrels using a high-speed camera to calculate their average velocities and kinetic energies (Fig. 7a–c). The propulsion performances of the bullet-type projectiles generally improve with CM addition to the Al/CuO-based EMs (Fig. 7d and e). The average velocities and kinetic energies



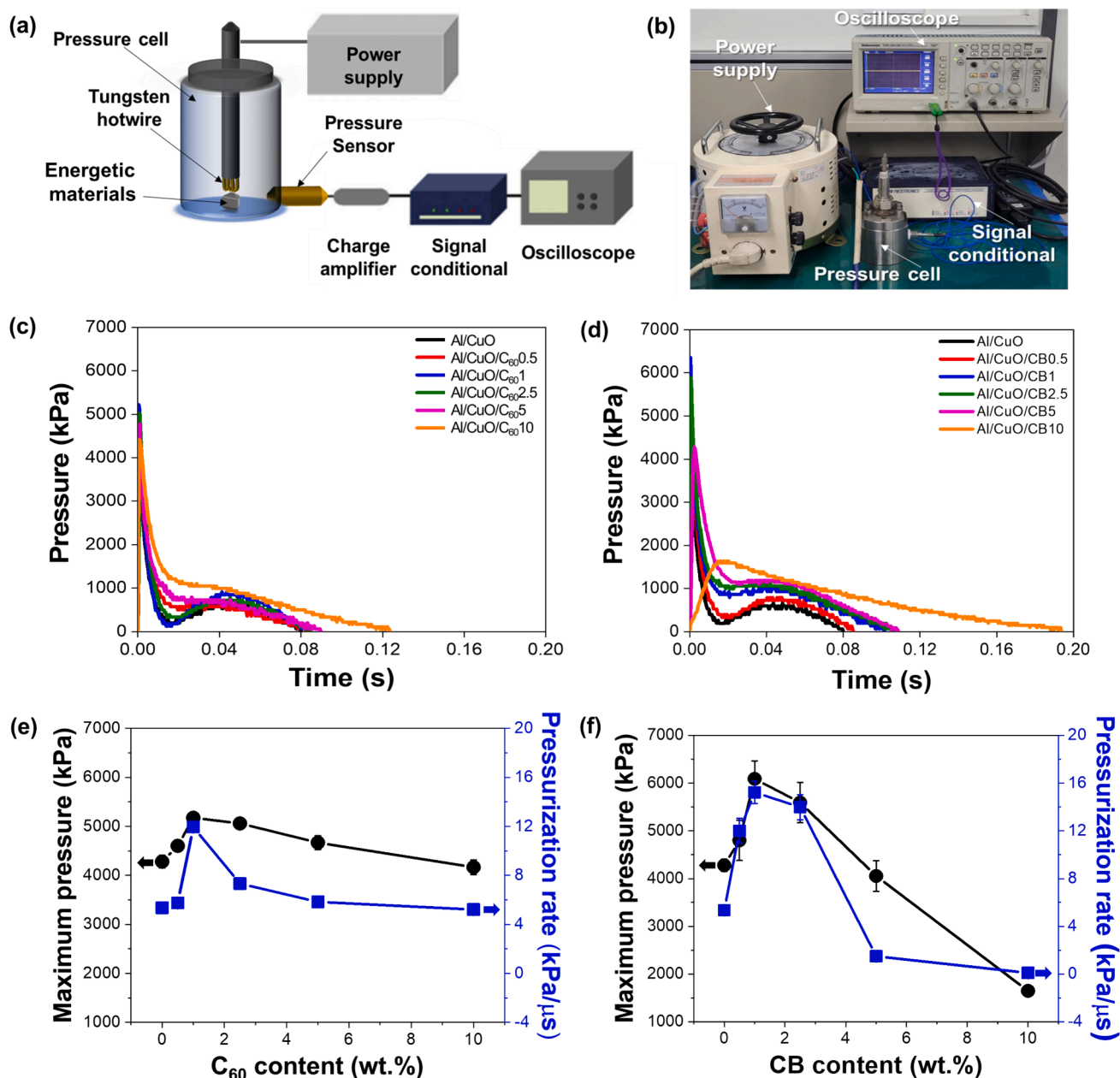
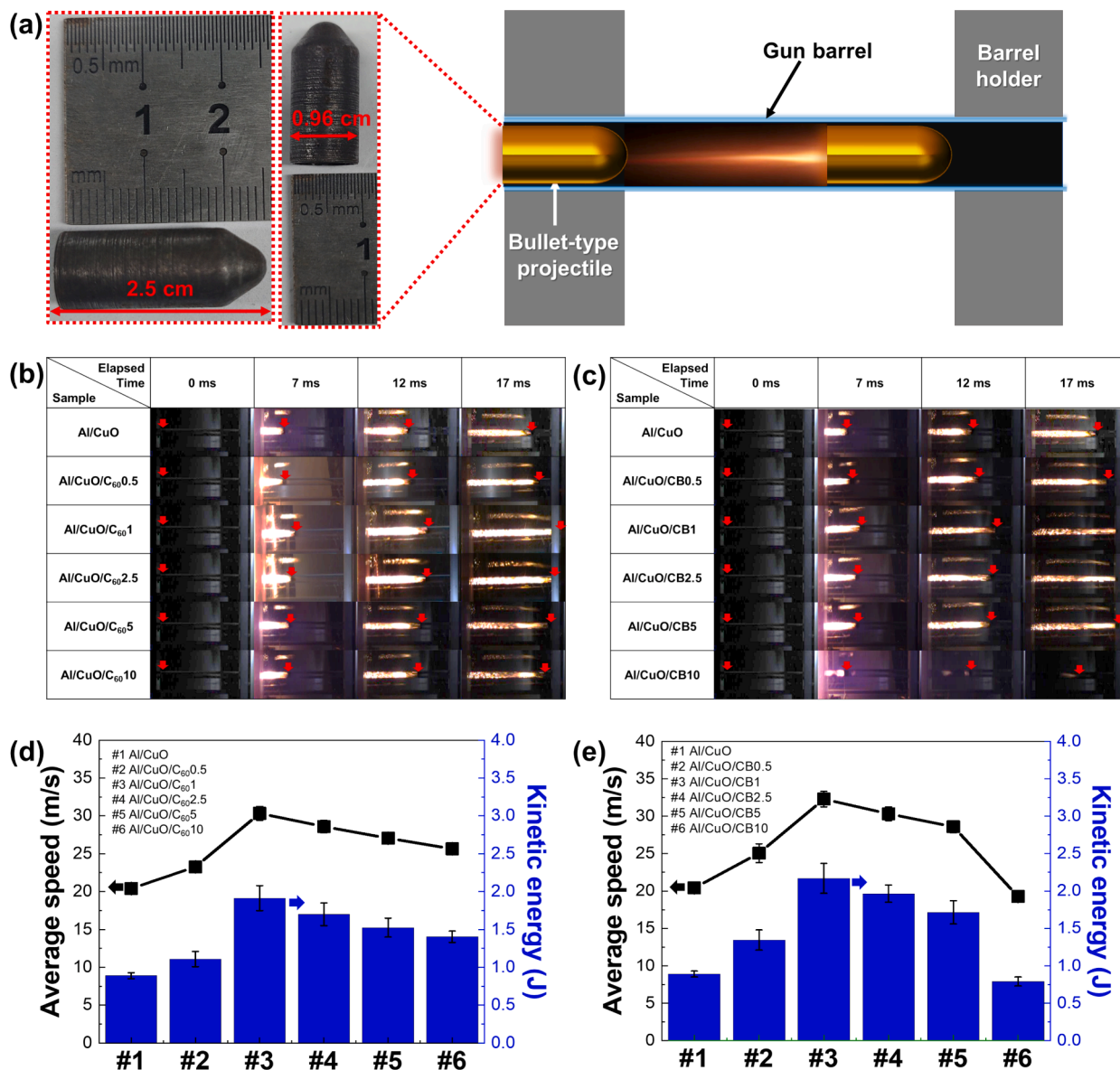


Fig. 6. (a) Schematic and (b) photograph of pressure cell tester system, and explosion-induced pressure traces of Al/CuO-based energetic materials (EMs) with various amounts of (c) fullerene (C<sub>60</sub>) and (d) carbon black (CB) additives, and the maximum pressures and pressurization rates of the Al/CuO-based EMs with various amounts of (e) C<sub>60</sub> and (f) CB additives.

of the projectiles increase significantly and linearly with the addition of 1 wt% CM and then gradually decrease with further addition. These trends are similar to the changes in the burn rates and explosion pressures of the EMs with various amounts of CM. Critically, CB addition results in larger increases in the average velocities and kinetic energies of the bullet-type projectiles compared to those observed following the addition of C<sub>60</sub> at the same concentrations. This is attributed to the superior thermal properties of CB compared to those of C<sub>60</sub>, which enhance the propulsion performances during the combustion of the EMs. Additionally, these findings suggest that the average velocities and kinetic energies of various bullet-type projectiles can be appropriately controlled by the types and amounts of the CMs within the Al/CuO-based EMs.

We also conducted rocket-type projectile propulsion studies to observe the changes in thrust generated by the traditional solid propellant KNSU (i.e., KNO<sub>3</sub>/C<sub>12</sub>H<sub>22</sub>O<sub>11</sub>) powder when the Al/CuO/CM-

based EMs were added. In these rocket-type projectile studies, a fixed mass ratio of KNSU: Al/CuO/CM = 96: 4 was used, and the materials were mechanically mixed using a ball mill. A schematic of the thrust measurement apparatus installed in the wind tunnel (30 × 30 × 200 cm) is shown in Fig. 8a. The prepared KNSU-Al/CuO/CM-based EMs is packed into the combustion chamber of a rocket projectile. Upon ignition, strong combustion flames and intense exhaust gases are observed. Real-time thrust curves are generated by connecting a load cell and data transmission, recording, and computer devices to a rocket-type projectile combustion chamber fixture, and the maximum thrust and specific impulse are determined based on these curves (Fig. 8b and c). The area under the thrust curve is defined as the total impulse, and the specific impulse is calculated by dividing the total impulse by the mass of the mixture. Additionally, high-speed camera measurements of the combustion chamber and flames were collected during rocket ignition. They show that the combustion flame and exhaust gases emitted from the



**Fig. 7.** (a) Image of a bullet-type projectile and a schematic of the propulsion evaluation system, and still images of the ballistic studies of projectiles charged with the (b) fullerene (C<sub>60</sub>)- and (c) carbon black (CB)-doped Al/CuO energetic materials EMs (Note: The red arrows indicate the locations of the bullet-type projectiles propelled by the EMs over time). The average speeds and kinetic energies of bullet-type projectiles charged with the (d) C<sub>60</sub>- and (e) CB-doped Al/CuO EMs. (For interpretation of the references to colour in this figure legend, the reader is referred to the web version of this article.)

combustion chamber exit increase in intensity over time when using KNSU with added Al/CuO/CM-based EMs compared to those observed using pure KNSU (Fig. 8d). The levels of maximum thrust and specific impulse are summarized in Fig. 8e and f. The maximum thrust and specific impulse can be increased by up to ~30- and ~7-fold using KNSU with added Al/CuO/CM-based EMs compared to those observed using pure KNSU. Notably, the highest levels of maximum thrust and specific impulse are consistently observed when 1 wt% CM is added to the Al/CuO-based EMs in the KNSU propellants, with general decreases in maximum thrust and specific impulse observed when their CM contents are >1 wt%. These trends can be inferred based on the burn rates and explosion pressures of the EM powders. The burn and pressurization rate and explosion pressure ranges of the Al/CuO/CM-based EMs significantly exceed those of KNSU (i.e., the combustion and pressurization rates and maximum explosion pressure of KNSU are ~0.004 m/s, ~0.008 kPa/s, and ~1216.55 kPa, respectively). Therefore, the application of Al/CuO/CM-based EMs as combustion promoters to traditional KNSU solid propellants can enhance their propulsion performances. The

Al/CuO/CM-based EMs were used as the primary propellants in the bullet-type projectiles, whereas they were used in small quantities as combustion promoters for the primary KNSU propellant in the rocket-type projectiles. Clearly, CB addition significantly enhances the propulsion characteristics of the bullet-type projectiles compared to those observed following C<sub>60</sub> addition. The overall amount of CM is lower compared to that of the primary KNSU propellant in a rocket-type projectile. Therefore, the enhancement in propulsion performance with CB addition is higher compared to that observed following C<sub>60</sub> addition but still lower than the enhancement observed when the Al/CuO/CM-based EM is used as the primary propellant in a bullet-type projectile. Ultimately, when comparing the various results of this study, it is suggested that the drastic change in combustion and propulsion characteristics of the EMs before and after the optimal amount of CM addition is closely related to the change in heat release (or energy density) based on the amount of CM added in Al/CuO-based EMs, as fundamentally confirmed in the DSC results.

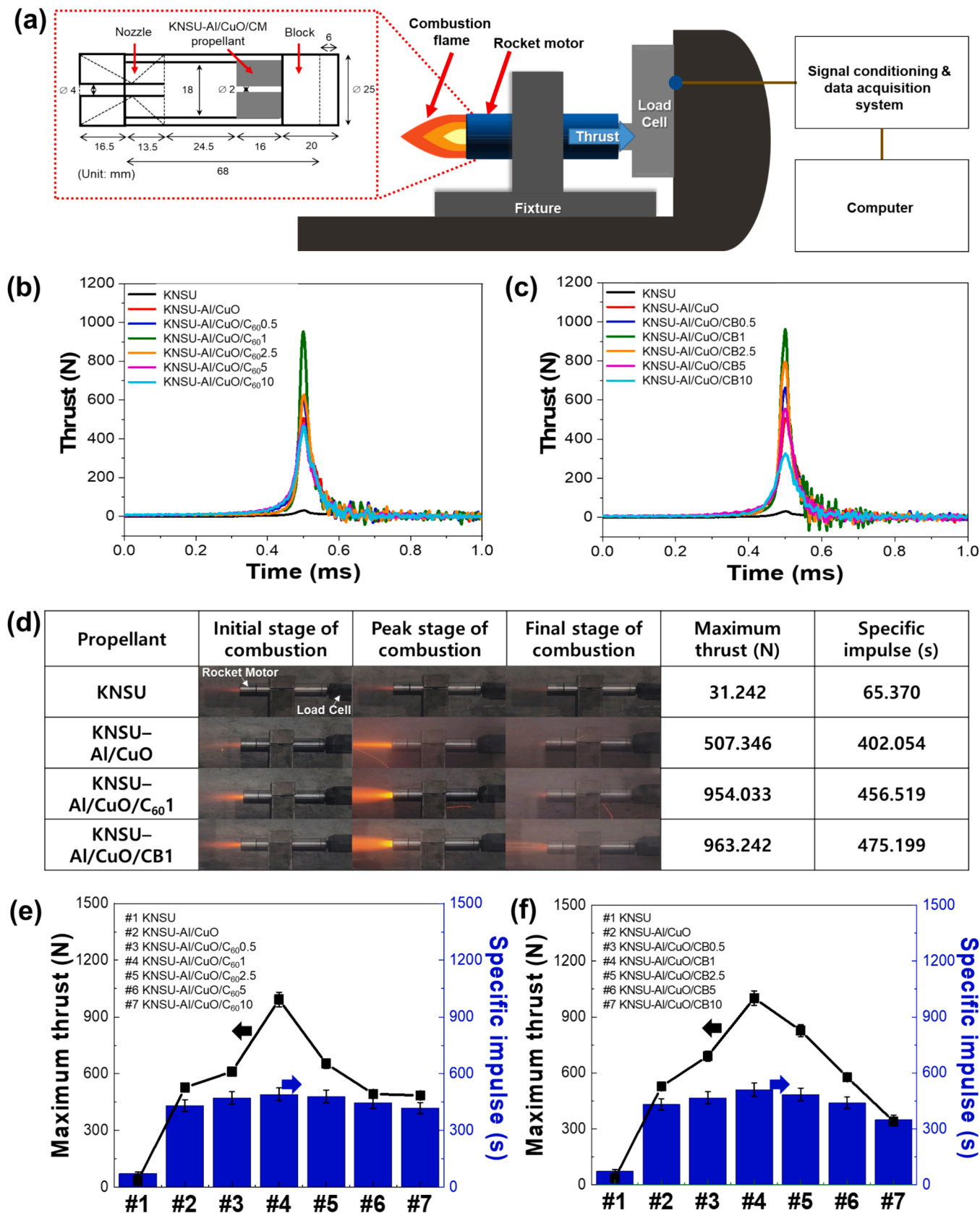


Fig. 8. (a) Schematic of the thrust evaluation system for rocket-type projectiles and the measured thrust curves of the (b) KNSU-Al/CuO/C<sub>60</sub>- and (c) KNSU-Al/CuO/CB-based propellants. (d) Still images of the combustion flames and exhaust plumes, and the levels of maximum thrust and specific impulse values generated by the rocket motors charged with the (e) various KNSU-Al/CuO/C<sub>60</sub>- and (f) KNSU-Al/CuO/CB-based propellants. (KNSU, KNO<sub>3</sub>: C<sub>12</sub>H<sub>22</sub>O<sub>11</sub> = 65: 35 wt% and KNSU: Al/CuO/carbon material = 96: 4 wt%).



#### 4. Conclusion

This study investigated the effects of CM addition on the ignition, combustion, and propulsion characteristics of Al/CuO-based EMs. We selected the representative CMs (i.e., C<sub>60</sub> and CB) and incorporated them into Al/CuO-based EMs. The total heat release of the Al/CuO-based EMs increased with CM addition to a certain level ( $\leq 1$  wt%), but the addition of excess CM ( $> 1$  wt%) led to a decrease in heat release. Additionally, although the sensitivity to electrical shock of the EMs increased with increasing CM content, its resistances to friction and mechanical shock improved. This was attributed to the higher electrical conductivity of the CM, which facilitated the rapid transmission of electrical shocks, whereas its increased mechanical elasticity absorbed and decelerated mechanical shocks. Therefore, to enhance the handling safeties of EMs, carefully determining the optimal amount of CM is crucial. The burn rates and explosion pressures of the Al/CuO-based EMs increased at levels of CM addition of  $\leq 1$  wt%, but declined sharply when the CM contents were  $> 1$  wt%. This suggested that an appropriate amount of CM promoted the aluminothermic reaction during ignition, whereas excessive CM addition impeded it. Based on the experimental total heat release, electrical and mechanical shock sensitivities, burn rate, and explosive pressure, CB (which displays a superior thermal conductivity compared to that of C<sub>60</sub>) significantly enhanced the ignition and combustion characteristics of the Al/CuO-based EMs when added in optimal amounts. Furthermore, we conducted small-scale bullet- and rocket-type projectile studies to evaluate the effects of these improvements on propulsion performance. The optimal amount of CM led to an increased average velocity and kinetic energy in the bullet-type projectile studies and an enhanced thrust and specific impulse in the rocket-type projectile studies. However, an excessive CM content ( $> 1$  wt%) caused sharp deteriorations in these propulsion characteristics. Thus, incorporating the optimal amount of a CM with an excellent thermal conductivity can improve the handling safety and enhance the ignition, combustion, and propulsion characteristics, enabling the design of EMs for use in thermal engineering applications.

#### Author contributions

A. Basyir and H. S. Kim contributed equally to this work as first authors. The manuscript was written with contributions from all authors, and all authors approved the final version.

#### CRediT authorship contribution statement

**Abdul Basyir:** Writing – original draft, Visualization, Methodology, Investigation. **Ho Sung Kim:** Writing – original draft, Investigation, Data curation. **Jung Keun Cha:** Visualization, Investigation. **Soo Hyung Kim:** Writing – review & editing, Visualization, Validation, Supervision, Project administration, Methodology, Funding acquisition, Conceptualization.

#### Declaration of competing interest

The authors declare that they have no known competing financial interests or personal relationships that could have appeared to influence the work reported in this paper.

#### Acknowledgments

This research was supported by grants from the National Research Foundation of the Republic of Korea, funded by the Ministries of Science and ICT (Grant No. RS-2023-00284622) and Education (Grant No. 2020R111A3061095). This research was also partially supported by the Korea Planning & Evaluation Institute of Industrial Technology and funded by the government of the Republic of Korea (Ministries of Trade, Industry, and Energy; Science and ICT; and the Interior and Safety;

National Fire Agency; Project Number: 1761002860).

#### Data availability

Data will be made available on request.

#### References

- [1] Trache D, Deluca LT. Nanoenergetic materials: preparation, properties, and applications. *Nanomaterials* 2020;10:2347.
- [2] Kim SB, Kim KJ, Cho MH, Kim JH, Kim KT, Kim SH. Micro- and nanoscale energetic materials as effective heat energy sources for enhanced gas generators. *ACS Appl Mater Interfaces* 2016;8:9405–12.
- [3] Sikder AK, Sikder N. A review of advanced high performance, insensitive and thermally stable energetic materials emerging for military and space applications. *J Hazard Mater A* 2004;112:1–15.
- [4] Anniyappan M, Talawar MB, Sinha RK, Murthy KPS. Review on advanced energetic materials for insensitive munition formulations. *Combust Explos Shock Waves* 2020;56:495–519.
- [5] Xu R, Xu J, Xue Z, Yan Q-L. Combustion performance modulation and agglomeration inhibition of HTPB propellants by fine Al/oxidizers integration. *Fuel* 2024;367:131587.
- [6] Ouyang K, Cheng J, Zhang Z, Li F, Ye Y, Shen R. Enhancing the combustion and propulsion performance of Al/CuO via introducing AlH<sub>3</sub> as fuel substitute. *Fuel* 2023;347:128483.
- [7] Comet M, Martin C, Schnell F, Spitzer D. Nanothermites: a short review - Factsheet for experimenters, present and future challenges. *Propellants Explos Pyrotech* 2019;44:18–36.
- [8] He W, Liu PJ, He GQ, Gozin M, Yan QL. Highly reactive metastable intermixed composites (MICs): preparation and characterization. *Adv Mater* 2018;30:1706293.
- [9] Pang W, Fan X, Wang K, Chao Y, Xu H, Qin Z, et al. Al-based nano-sized composite energetic materials (nano-CEMs): preparation, characterization, and performance. *Nanomaterials* 2020;10:1–22.
- [10] Ahn JY, Kim JH, Kim JM, Lee DW, Park JK, Lee D, et al. Combustion characteristics of high-energy Al/CuO composite powders: the role of oxidizer structure and pellet density. *Powder Technol* 2013;241:67–73.
- [11] Yan QL, Gozin M, Zhao FQ, Cohen A, Pang SP. Highly energetic compositions based on functionalized carbon nanomaterials. *Nanoscale* 2016;8:4799–851.
- [12] Zhang T, Gao X, Li J, Xiao L, Gao H, Zhao F, et al. Progress on the application of graphene-based composites toward energetic materials: a review. *Def Technol* 2024;31:95–116.
- [13] Pang W, Xia X, Zhao Y, Deluca LT, Trache D, Ouyang D, et al. Effect of carbon nanotubes (CNTs) on the performance of solid rocket propellants (SRPs): a short review. *FirePhysChem* 2023;3:227–33.
- [14] Pal Y, Palateerdham SK, Mahottamananda SN, Sivakumar S, Ingenito A. Combustion performance of hybrid rocket fuels loaded with MgB<sub>2</sub> and carbon black additives. *Propul Power Res* 2023;12:212–26.
- [15] Han X, Wang TF, Lin ZK, Han DL, Li SF, Zhao FQ, et al. RDX/AP-CMDB propellants containing fullerenes and carbon black additives. *Def Sci J* 2009;59:284–93.
- [16] Jin B, Peng R, Chu S, Huang Y, Wang R. Study of the desensitizing effect of different [60] fullerene crystals on cyclotetramethylenetetranitramine (HMX). *Propellants Explos Pyrotech* 2008;33:454–8.
- [17] Wang H, Kline DJ, Renwoldt MC, Zachariah MR. Carbon fibers enhance the propagation of high loading nanothermites: in situ observation of microscopic combustion. *ACS Appl Mater Interfaces* 2021;13:30504–11.
- [18] Jiang Y, Deng S, Hong S, Tiwari S, Chen H, Nomura K, et al. Synergistically chemical and thermal coupling between graphene oxide and graphene fluoride for enhancing aluminum combustion. *ACS Appl Mater Interfaces* 2020;12:7451–8.
- [19] Shen J, Qiao Z, Wang J, Yang G, Chen J, Li Z, et al. Reaction mechanism of Al-CuO nanothermites with addition of multilayer graphene. *Thermochim Acta* 2018;666:60–5.
- [20] Su J, Hu Y, Zhou B, Ye Y, Shen R. The role of graphene oxide in the exothermic mechanism of Al/CuO nanocomposites. *Molecules* 2022;27:1–17.
- [21] Chen L, Yanling L, Weibo Y, Ran Z, Shiguo D, Ke N. Self-assembly preparation and thermal decomposition of Al/CuO/graphene oxide. *IOP Conf Ser: Earth Environ Sci* 2021;680:012081.
- [22] Saha D, Deng S. Hydrogen adsorption on partially truncated and open cage C60 fullerene. *Carbon* 2010;48:3471–6.
- [23] Kini KA. Surface area of active carbon and carbon black by the BET method using argon, carbon dioxide, methanol, krypton, and xenon. *J Phys Chem* 1964;68:217–8.
- [24] Monogarov KA, Meerov DB, Fomenkov IV, Pivkina AN. Energy transferred to energetic materials during impact test at reaction threshold: look back to go forward. *FirePhysChem* 2023;3:255–62.
- [25] Klapotke TM, Lemarchand G, Lenz T, Muhlemann M, Stierstorfer J, Weber R. Impact and friction sensitivities of PETN: I. sensitivities of the pure and wetted material, propellants, explosives. *Pyrotechnics* 2022;47:e202200150.
- [26] Picheau E, Amar S, Derre A, Penicaud A, Hof F. An introduction to the combustion of carbon materials. *Chem-A Eur J* 2022;28:e202200117.
- [27] Lee SM, Lee SH, Roh JS. Analysis of activation process of carbon black based on structural parameters obtained by XRD analysis. *Crystals* 2021;11:153.

- [28] Papirer E, Brendle E, Ozil F, Balard H. Comparison of the surface properties of graphite, carbon black and fullerene samples, measured by inverse gas chromatography. *Carbon* 1999;37:1265–74.
- [29] Ivetic M, Mojovic Z, Matija L. Electrical conductivity of fullerene derivatives. *Mater Sci Forum* 2003;413:49–52.
- [30] Marinho B, Ghislandi M, Tkayla E, Koning CE, With G. Electrical conductivity of compacts of graphene, multi-wall carbon nanotubes, carbon black, and graphite powder. *Powder Technol* 2012;221:351–8.
- [31] Weir C, Pantoya ML, Ramachandran G, Dallas T, Prentice D, Daniels M. Electrostatic discharge sensitivity and electrical conductivity of composite energetic materials. *J Electrostat* 2013;71:77–83.
- [32] Saito K, Miyazawa K, Kizuka T. Bending process and Young's modulus of fullerene C60 nanowhiskers. *Jpn J Appl Phys* 2009;48:010217.
- [33] Habis NA, Moumen AE, Tarfaoui M, Lafdi K. Mechanical properties of carbon black/poly ( $\epsilon$ -caprolactone)-based tissue scaffolds. *Arab J Chem* 2020;13:3210–7.
- [34] Shen J, Wang H, Kline DJ, Yang Y, Wang X, Rehwoldt M, et al. *Combust Flame* 2020;215:86–92.